

Do not type or paste anything outside this line. Type up to, but not beyond, this line on page 1 of a two-page manuscript.

## Cortical control for prosthetic devices

A.B. Schwartz, D.W. Kipke and P.D. Perepelkin

Arizona State University, Dept. of Chemical, Biological and Materials Engineering  
Tempe, AZ 85287-6006

### ABSTRACT

The work presented in this session is part of a project to develop an arm-control system based on neuronal activity recorded from the cerebral cortex. This will make it possible for amputees or paralyzed individuals to move a prosthetic arm or, using functional neural stimulation, their own limbs as effortlessly and with as much skill as intact individuals. We are developing and testing this system in monkeys and hope to have a prototype working in the next couple of years. This project has been made more feasible because we have been able, in the last 15 years to extract, from the brain, a signal that represents arm trajectory accurately. In this paper, we will describe how this technique was developed and how we will use this as the basis for our control signal. An alternative approach using a self-organizing feature map, an algorithm to deduce arm configuration given an endpoint trajectory and the development of a telemetry system to transmit the neuronal data will be described in subsequent papers.

Keywords: cerebral cortex, neurophysiology, population vector, biological control signal, prosthetics

### 1. POPULATION VECTOR ALGORITHM

The technique we use to transform neuronal firing rates to spatiotemporal arm trajectories is referred to as the population vector algorithm (PVA). This signal is recorded from the shoulder-elbow area of the primary motor cortex, a region of the frontal lobe intimately associated with voluntary movements. Microelectrodes capable of recording action potentials from single cells are used to intercept the electric fields generated by these impulses. The rate that a single cell generates action potentials (its firing rate) is the parameter upon which the PVA is based.

The PVA is based on the initial finding by Georgopoulos and colleagues<sup>1</sup> that the direction of the hand during multi-joint arm movements is represented by a simple relation with the discharge rate of motor cortical cells. This "tuning" function is broad and spans all movement directions, suggesting that many cells represent a given direction simultaneously. The primary descriptor of this function is the movement direction in which a cell fires at its maximal rate--the "preferred" direction. The nature of the tuning suggests that a population of motor cortical cells is capable of encoding uniquely and accurately the movement direction of the hand. This hypothesis has been proven for two- and three dimensional movements<sup>2,3,4</sup>. For each cell, a unit

Do not type or print anything inside the line. Type inside, but not beyond, the line margin. Leave a 1 cm wide right vector in that cell's preferred direction is multiplied by its average discharge rate during the movement. This weighting is done on all the vectors pointing in the preferred directions of the different cells to be included in the population. The weighted vectors are summed and the resulting "population vector" points accurately in the movement direction.

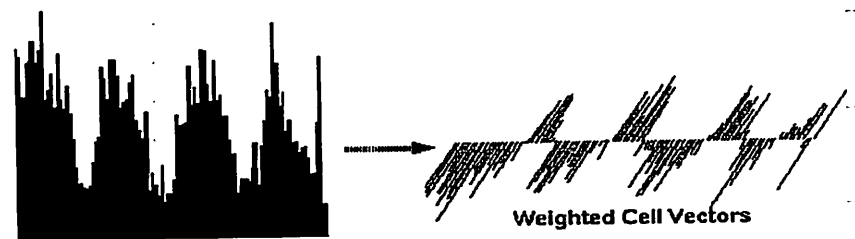
### Figure 1. Population vector algorithm.

**A.** Rasters derived from the "center->out" task were used to calculate a cell's preferred direction. Each raster represents five repetitions of a movement from the center of the figure to a target located at the raster's position. Each raster is aligned to movement onset. The average discharge rate during the reaction and movement time was greatest for movements down and to the left. The preferred direction of this unit was  $254^\circ$  and is represented by the arrow in the middle of the figure. This procedure yields a unit vector pointing in the cell's preferred direction.

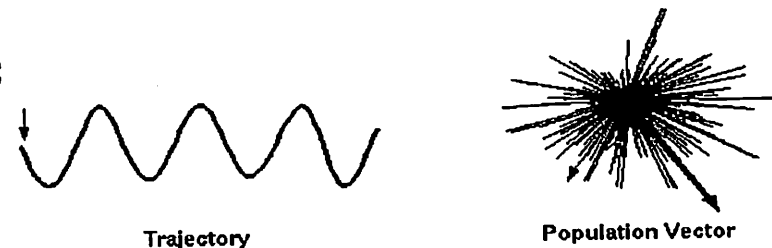
#### A Center->out Task



#### B Tracing Task



#### C



**B.** The instantaneous discharge rate of this cell was calculated in 100 bins as a sinusoid was traced and is represented in the histogram. Spike data were aligned to a sync point 120 ms before the finger exited the start target. The unit vector was multiplied by the discharge rate. The geometric mean rate was calculated over all movements and subtracted from the weighted cell vector for each bin.

**C.** The same procedure was carried out for all 554 cells in the population. The result for the first bin of this sinusoid task is represented as a cluster of cell vectors. The population vector (not to scale) resulting from the vector addition of the 554 cells is represented as the heavy arrow. The small arrow shows the vector contribution of the unit displayed in A and B. The direction of the population vector matches the initial direction of the trajectory.

Do not type or paste anything outside this line. Type up to, but not beyond, the blue margin lines at left and right.

Initially this algorithm was applied to point-to-point movements and the discharge rate was averaged over the entire movement, a valid simplification since the directions were straight. Recently, there has been a large body of work<sup>5-15</sup> showing that the trajectory of the hand as it moves during a behavioral task follows rules suggesting that the hand path is the overriding feature of movement controlled by the CNS. We showed originally that a time series of population vectors added tip-to-tail accurately represents 3D point to point movements<sup>4</sup> (Fig. 1). Schwartz<sup>16-20</sup> developed a set of drawing tasks and modified the PVA to determine how motor cortical activity is related in an ongoing fashion to the evolution of a movement as it takes place.

### 1.2 Tuning parameters of individual neurons

The characteristic directional tuning of each neuron will be determined from the averaged neuronal discharge rates found in the center->task in which the animal moves in radial directions from a center start point.

The tuning equation used to describe a neuron's directionality is:

$$D = b_0 + b_x \cos \alpha + b_y \cos \beta + b_z \cos \gamma.$$

D is the discharge rate of the neuron when the animal is moving its arm in a direction with an angle  $\alpha$  to the x axis and angle  $\beta$  to the y axis and angle  $\gamma$  to the z axis. This direction can be represented by a movement vector  $\mathbf{M}$  with components  $m_x = \cos \alpha$ ,  $m_y = \cos \beta$  and  $m_z = \cos \gamma$ .

This leads to:

$$D = b_0 + b_x m_x + b_y m_y + b_z m_z \tag{1}$$

A multiple regression is carried out to find  $b_0$ ,  $b_x$ ,  $b_y$  and  $b_z$  over the data consisting of the average discharge rate, D, from the trials to the eight different targets. An  $r^2$  corresponding to a p value  $< .01$  is used as the criterion for assessing whether the data fit the equation.

If Eq. 1 is changed to:

$$D - b_0 = b_x m_x + b_y m_y + b_z m_z \tag{2}$$

we can easily see that it fits the dot product expression;

$$\mathbf{B} \cdot \mathbf{M} = b_x m_x + b_y m_y + b_z m_z \tag{3}$$

if we assume there exists a vector  $\mathbf{B}$  that points in the cell's preferred direction with components  $b_x$ ,  $b_y$ , and  $b_z$ .

This can be pictured more clearly if Eq. 3 is expanded further according to the dot product definition:

$$\mathbf{B} \cdot \mathbf{M} = b_x m_x + b_y m_y + b_z m_z = |\mathbf{B}| |\mathbf{M}| \cos \Theta \tag{4}$$

$\Theta$  is the angle between the movement vector and the cell's preferred direction. Note that if the movement is in the cell's preferred direction that  $\Theta = 0$  and  $\cos \Theta = 1$ .

Do not type or paste anything outside this line. Type up to, but not beyond, the thick margin lines at left and right.

Combining equations 2 and 4 and remembering that  $|M| = 1$  we see that:  $D_{\text{pref}} - b_0 = |B|$ . The magnitude of  $B$ ,  $|B|$ , is equal to  $(b_x^2 + b_y^2 + b_z^2)^{1/2}$ . Thus the difference between the cell's maximum rate of discharge,  $D_{\text{pref}}$ , and the average rate of discharge over all movements,  $b_0$ , is equal to the magnitude of the cell vector,  $|B|$ .

### 1.3 Population coding

Using only the preferred direction of a neuron, its contribution to the population response will be determined based on its observed firing rate at an instant in time. This contribution can be conceptualized as a vector  $N_{ij}$  in the cell's preferred direction with a magnitude  $w_{ij}$ , proportional to the cell's discharge rate at time point  $j$ .

For an individual cell  $i$  and a particular bin  $j$ :

$$C = B/|B|$$

$$N_{ij} = w_{ij} C_i$$

$$w_{ij} = D_{ij} - G_i$$

$N_{ij}$  is the cell vector for cell  $i$  of the  $j$ th bin contributing to the population response. A weighting factor,  $w_{ij}$  is assigned to the  $j$ th bin,  $G_i$  is the geometric mean taken over all of the spikes in the run and  $C_i$  is a constant unit vector pointing in the cell's preferred direction. Thus the contribution of a particular cell to the population is always in the same direction, but the magnitude of the contribution will change bin by bin.

$$\text{ipv}_j = P_j = \sum_{i=1}^n N_{ij}$$

The instantaneous population vector (ipv) for the  $j$ th bin is formed by summing all the cell vectors ( $i = 1, n$ ) from the  $n$  simultaneously recorded cells contributing to the population for time instant  $j$ . The ipv serves as the output of the system signal transformation system. This represents the instantaneous direction and magnitude of the end of the arm.

## 2. Results

Our findings, based on this algorithm, show that the trajectory of the hand is well represented in the cortical activity and that the shape of the drawn figure is represented in this activity. Furthermore several of the behavioral invariants characterizing adult human movements are also well represented in this activity (Fig. 2).

Do not touch the screen with your finger. Turn on the light and hold the pen in your right hand. The screen is on the right.

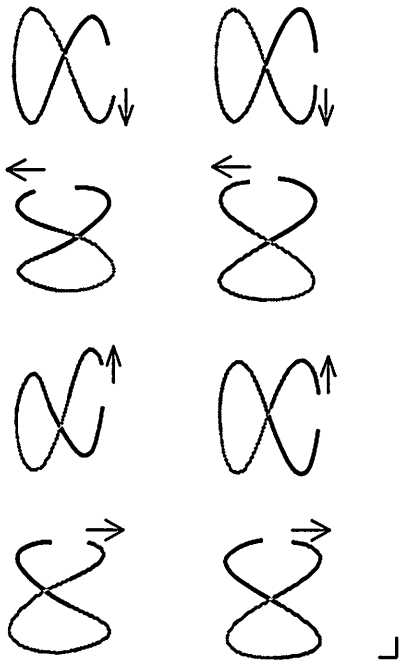


**Figure 2.** Neural and actual trajectory comparison during lemniscate drawing. Four different lemniscates were drawn. The neural trajectories, created by adding 100 sequential ipvs tip-to-tail are on the left. Corresponding arm trajectories measured at the finger are on the right. These data were recorded as two monkeys drew figure-eights on a touch screen. The neural trajectories were constructed with the responses of 325 cells from both monkeys. The match between the neural prediction and the actual movement is extremely good for the four different lemniscates, regardless of the direction they were drawn or their orientation. The figures were produced in four segments (indicated by the different colors) as is the case when humans draw the same figures.

One such invariant is the  $2/3$  power law originally described for handwriting. This law has been found to be a robust relation for many kinds of drawing movements<sup>21</sup>. These findings show that path curvature to the  $2/3$

power is linearly related to the angular velocity of the hand. This relation is variable for children but stabilizes at the age of twelve<sup>22,23</sup>. We have found that our monkeys follow this law when drawing objects<sup>18,20</sup> (Fig. 3). Furthermore, the neural trajectory calculated using the PVA with motor cortical activity, also follows this relation showing that this psychophysical observation is based on CNS processing.

Another behavioral finding relating to the time course and displacement of the hand is that of segmentation. The apparently continuous movements found in graceful drawing and reaching behaviors is actually made of segments defined by zero crossings in angular or linear velocity<sup>8,24</sup>. This is related to the  $2/3$  power law because such segments are clearly delineated in curvature vs. velocity plots where the slopes change instantaneously. We have found that when monkeys generate closed figures such as figure-eights, that they produce the same segmentation as human subjects. The segments are represented in the neural trajectories. Interestingly, if the prediction interval (time between a point in the neural trajectory and the corresponding point in the actual trajectory) is calculated throughout the task a correspondence between this measure and the

segments is observed (Fig. 2). This suggests that segmentation is a key feature of the movement generation process. Linked with the 2/3 power law observation this suggests that smooth, coordinated movements are generated by merging segments together where path curvature is minimal and hand speed is high. It is clear from our work, that hand trajectory is not only clearly represented in the motor cortex, but that the behavioral invariants characteristic of anthropoid movement are incorporated in this signal as well.

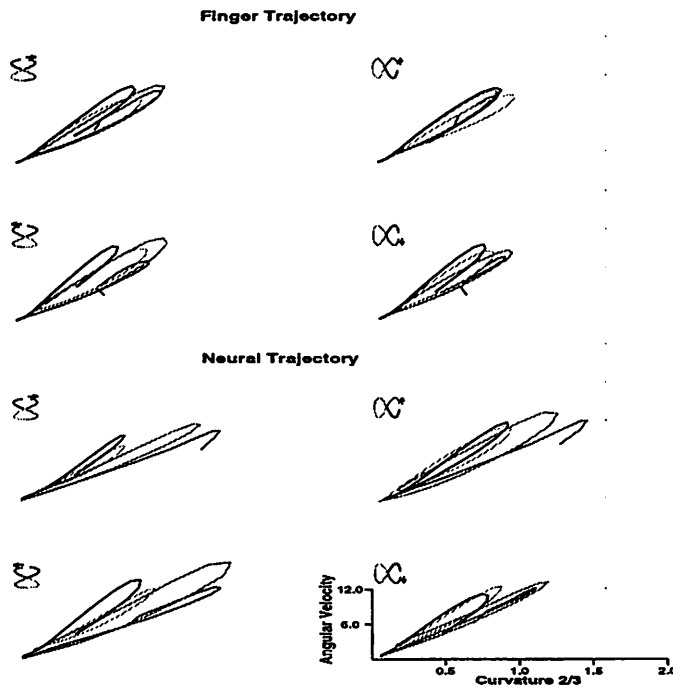


**Figure 3. Two-thirds power law representation in motor cortical activity. Angular velocity is plotted against curvature to the 2/3 power. The relation is linear--showing that monkeys obey the same rule as human adults. The relation is linear for the neural data as well, showing that this invariant is incorporated in the motor cortical activity. Furthermore, segments are separated at the origin of the plot (colors correspond to the segments of the previous figure) for both sets of neural data, another finding in common with those from human psychophysical experiments.**

We feel that it is essential to use this type of signal to control prosthetic arms in a way that will be useful and acceptable enough for the user to justify implanting a chronic cortical electrode array.

### 3. Recording technology

One aspect of the technology that has limited us, is the ability to record large numbers of action potentials from individual cells simultaneously. The results generated to this point were from experiments in which single units were isolated one-at-a-time. The animal would perform the same task each time a different unit was isolated and the data collapsed across trials. The data used to generate a single population vector were often collected from the right and left sides of multiple animals. Obviously, if we are to use this technique to generate population vectors in

Do not type or paste anything outside this line. Type up to, but not beyond, the blue margin lines at left and right

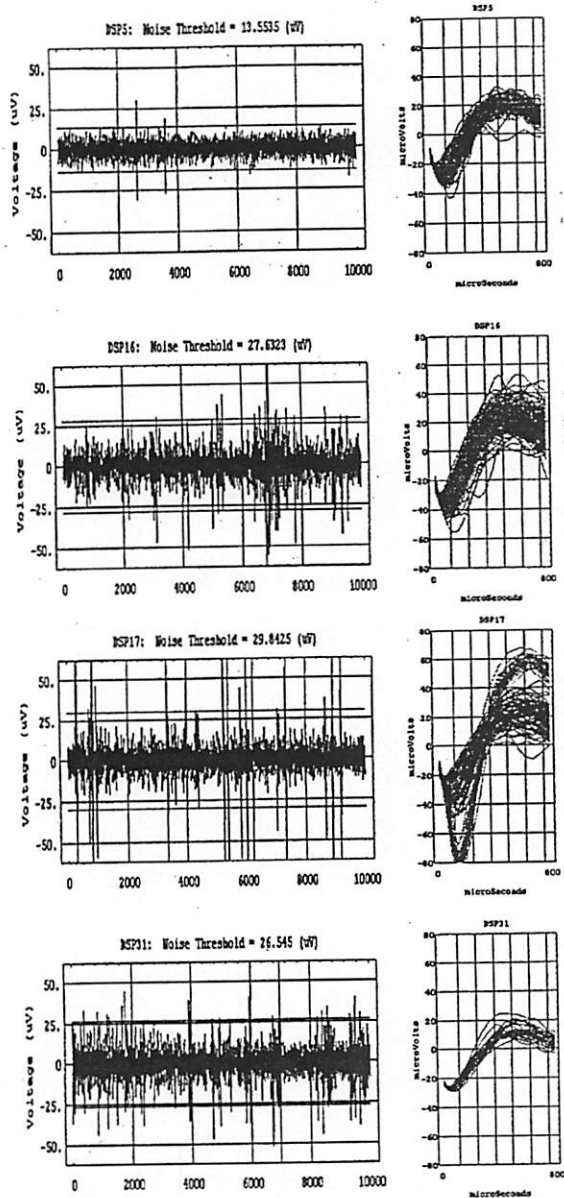


Figure 4. Example of four channels of recorded spikes. Traces on the left show a one second period of activity. Those on the right show superimposed waveforms of discriminated units. Channels 5 and 16 each show one clear unit. Channel 5 has a small amount of noise, while 16 is rather noisy, with one spike that stands out. Three spikes can be separated in channel 17. No single units can be discriminated from the multi-unit activity of channel 31.

realtime, it will be necessary to record a population of units simultaneously.

Various types of electrodes have been designed to record multiple, single units simultaneously. We have found that arrays of microwires implanted permanently into the cortex to be successful in this regard. To date, we have made significant progress toward achieving this in both domestic cats and rhesus monkeys. We have implanted multichannel electrodes (an array of 32 microwires) into cerebral cortices of eight animals (seven cats and one monkey) and recorded simultaneous single-unit activity from several to 18 months in a majority of the animals. The cats were implanted as part of an early phase of the Whitaker project focusing on evaluating electrodes and developing surgical and recording procedures. In these animals, we

typically observe well-isolated single unit activity on at least 25% of the channels (Fig. 4). In addition, many of the other channels exhibit multiunit ensemble activity, which may ultimately prove useful for augmenting single-unit activity in estimating finger velocity. The spike activity on many of the channels is relatively stable over extended periods of several months to over a year, as indicated by the consistency of spike waveforms. After the preparation has stabilized following implantation, the waveforms on an active channel may vary from day to day, but over weeks and months similarly shaped spike waveforms tend to remain. Implanting the electrodes does not seem to cause functional damage.

Do not type or paste anything outside this line. Type up to, but not beyond, the thin margin line on the right.

Our laboratory is constructed so that the two recording rooms where the animals will carry out the behavioral tasks are physically separate from the main lab where the investigators will monitor the signals. This allows the animals to work in an undisturbed environment. Sets of preamplifiers (16 channel FETs, NB Labs) are incorporated into the plug that mates to the electrode connector mounted on the skull. The other end of this three-foot cable is plugged into a signal conditioner unit that amplifies the signals before they are transmitted over a 30 foot shielded cable to the main recording setup. Our preliminary studies verify the fidelity of this recording system.

The neural recordings are processed with a 32-channel neural recording system from Spectrum Scientific (the Multichannel Neuronal Acquisition Processor system, or MNAP). For this project, we request an upgrade to our current system to allow simultaneous recording of 96 electrode channels. The MNAP system provides real-time, multi-channel discrimination and storage of spike waveforms and spike trains. It is a modular system which consists of a rack-mount chassis containing plug-in boards for amplification, filtering, and signal processing of extracellular recordings from the implanted electrodes. The neural signals are sampled at 40 kHz and real-time processing is accomplished by using multiple digital signal processors. The system is controlled by a Windows program running on a Pentium PC, which is connected to the plug-in boards through a high-speed bus. The PC provides the graphical user-interface for the system. The units are discriminated and the spike trains are saved to disk in real-time. This module can be programmed with different algorithms to select spikes. Presently, we are using a time-amplitude algorithm where the desired waveform must pass through two successive boxes (width is time and height is voltage) separated by a fixed time increment and centered as a fixed voltage. Other algorithms using principal components or templates can also be used. It is possible to discriminate three different waveforms reliably with each DSP. With our current system, the collection of 96 single spike trains would be the best case. In addition, PSTHs, average firing rates, and interval histograms are continuously calculated and displayed on the PC monitor to allow the recording session to be monitored closely.

The firing rates of all recorded units will be measured in 20 msec intervals and the ipv calculated for this bin. This ipv will serve as input to the next processing stage where inverse kinematic procedures will be used to determine the set of joint angles used to obtain an anthropomorphic configuration of the arm.

#### 4. ACKNOWLEDGEMENTS

This work was performed at the Whitaker Center for Neuromechanical Control and funded by the Whitaker Foundation. The authors would like to thank Barrow Neurological Institute and Arizona State University for Center support.



Do not write or print anything outside this line. Type up to, but not beyond, the blue margin lines at left and right.

## 5. REFERENCES

1. Georgopoulos AP, Kalaska JF, Caminiti R, Massey JT (1982) On the relations between the direction of two-dimensional arm movements and cell discharge in primate motor cortex. *J Neurosci* 2(11): 1527-1537
2. Georgopoulos AP, Caminiti R, Kalaska JF, Massey JT (1983) Spatial coding of movement: a hypothesis concerning the coding of movement direction by motor cortical populations. *Exp Brain Res Suppl.* 7: 327-336
3. Georgopoulos AP, Schwartz AB, Kettner RE (1986) Neuronal population coding of movement direction. *Science* 233: 1357-1440
4. Georgopoulos AP, Kettner RE, Schwartz AB (1988) Primate motor cortex and free arm movements to visual targets in three-dimensional space. II. Coding of the direction of movement by a neuronal population. *J Neurosci* 8: 2928-2937
5. Bizzi E, Accornero N, Chapple W, Hogan N (1982) Arm trajectory formation in monkeys. *Exp Brain Res* 46: 139-143
6. Soechting JF, Lacquaniti F (1981) Invariant characteristics of a pointing movement in man. *J Neurosci* 1: 710-720
7. Soechting JF, Ross B (1984) Psychophysical determination of coordinate representation of human arm orientation. *Neuroscience* 13: 595-604
8. Soechting JF, Terzuolo CA (1987b) Organization of arm movements. Motion is segmented. *Neuroscience* 23: 39-52
9. Soechting JF, Terzuolo CA (1987a) Organization of arm movements in three-dimensional space. Wrist motion is piece-wise planar. *Neuroscience* 23: 53-61
10. Soechting JF (1989) Elements of Coordinated Arm Movements in Three-Dimensional Space. In: Wallace SA (ed) Perspectives on the Coordination of Movement. Elsevier Science Publishers B.V., North-Holland, pp 47-83
11. Viviani P, Terzuolo C (1982) Trajectory determines movement dynamics. *Neuroscience* 7(2): 431-437
12. Lacquaniti F, Ferrigno G, Pedotti A, Soechting JF, Terzuolo C (1987) Changes in spatial scale in drawing and handwriting: kinematic contributions by proximal and distal joints. *J Neurosci* 7:3: 819-828
13. Fagg AH, Helms-Tillery SI, Terzuolo CA (1992) Velocity of motion influences the perception of hand trajectories in the absence of vision. *Soc Neurosci Abs* 18: 1551
14. Hocherman S, Wise SP (1989) Movement trajectory or goal representation in primate premotor and primary motor cortex. *Soc Neurosci Abs* 15: 789
15. Viviani P, Flash T (1995) Minimum-jerk, two-thirds power law, and isochrony: Converging approaches to movement planning. *J Exp Psy : Hum Per Perf* 21: 32-53
16. Schwartz AB (1992) Motor cortical activity during drawing movements. Single-unit activity during sinusoid tracing. *J Neurophysiol* 68: 528-541
17. Schwartz AB (1993) Motor cortical activity during drawing movements: Population response during sinusoid tracing. *J Neurophysiol* 70: 28-36
18. Schwartz AB (1994) Direct cortical representation of drawing. *Science* 265: 540-542

Do not type or paste anything outside this line. Type up to, but not beyond, the blue margin lines at left and right

19. Moran DW, Schwartz AB (1996) Motor cortical activity during drawing movements: Population representation during spiral tracing. *J Neurophysiol* (to be submitted)
20. Schwartz AB, Moran DW (1996) Motor cortical activity during drawing movements: Population representation during lemniscate drawing. *J Neurophysiol* (to be submitted)
21. Lacquaniti F, Terzuolo C, Viviani P (1983) The law relating kinematic and figural aspects of drawing movements. *Acta Psychol* 54: 115-130.
22. Sciaky R, Lacquaniti F, Terzuolo C (1987) A note on the kinematics of drawing movements in children. *J Mot Beh* 19:4: 518-525.
23. Viviani P, Schneider R (1991) A developmental study of the relationship between geometry and kinematics in drawing movements. *J Exp Psychol* 17:1: 198-218
24. Viviani P, Cenzato M (1985) Segmentation and coupling in complex movements. *J Exp Psychol* 11:6: 828-845